Int. J. Heat Mass Transfer. Vol. 28, No. 7, pp. 1393–1404, 1985
Printed in Great Britain

0017-9310/85 $3.00 + 0.00
Pergamon Press Ltd.

Experiences of a solar collector test method using Fourier transfer functions

W. KAMMINGA
Department of Applied Physics, University of Groningen, 9747 AG Groningen, The Netherlands

(*Received* 9 *July* 1984 *and in final form* 10 *December* 1984)

Abstract—A test method for collectors, essentially based on time-varying conditions has been developed. A finite Fourier transformation of the differential equations describing the collector, leads to relations for the collector characteristics. Because of errors, only a limited number of these equations defined by particular choices of both the time interval t_e and the Fourier variable ω, can be applied in the test method. The collector parameters can be determined by a least-square method using only one series of experimental measurements made by a fixed fluid inlet temperature. The results are comparable with those obtained from more series of measurements with different values of the fluid inlet temperatures.

1. INTRODUCTION

THE TESTING of solar collectors under stationary weather conditions according to the requirements of various outdoor or mixed outdoor/indoor test procedures, requires a long period of constant insolation. In moderate climates, the practical and efficient testing of collectors can be improved by methods based on transient weather conditions. A number of such methods are mentioned in literature (e.g. [1, 2]). They are based on more or less complicated relations between the useful energy, the insolation and the heat losses integrated over the time of the experimental measurements, derived from a heat balance of the collector.

The test method described in this paper, makes use of the well-known technique of the Fourier transform for solving time-dependent problems. A finite Fourier transform of the set of differential equations representing the mathematical model of the collector, results in a relation in the frequency domain.

Particular choices of the Fourier variable lead to a set of algebraic equations between the useful energy, the insolation and the heat losses. The collector characteristics of interest such as the absorptance–transmittance product and the heat loss resistance, follow by a least-square method. At first sight, one series of experimental measurements with a fixed fluid inlet temperature should be sufficient to determine the collector characteristics by taking a sufficient number of different Fourier variables. In practice, the method only works with particular choices of both the time interval t_e and the Fourier variable ω. As a first reason, we mention, the sensitivity for numerical errors in the calculations and experimental errors in the data. Secondly, the actual solar radiation received at the collector absorber shows dominant relatively low frequencies with dominant intensity variations. As described at the end of Section 5, convenient time intervals are partly determined by the ratio of t_e and the dominant period of the insolation.

Additionally, the method will be applied using several series of experimental measurements, each with a different fixed fluid inlet temperature. In this case, it suffices to take a limited number of the Fourier variable ω near zero for each series.

2. THE THEORETICAL MODEL OF THE TEST METHOD

The starting point is a mathematical model of the collector, consisting of a simple three-node model. The heat balance condition for the cover plate, the absorber and the circulating fluid, respectively, leads to the following set of differential equations:

$$C_g \frac{\partial T_g}{\partial t}(x,t) = \frac{T_a(t) - T_g(x,t)}{R_{ag}} + \frac{T_p(x,t) - T_g(x,t)}{R_{pg}} \quad (1)$$

$$C_p \frac{\partial T_p}{\partial t}(x,t) = \frac{T_g(x,t) - T_p(x,t)}{R_{pg}} + \frac{T_f(x,t) - T_p(x,t)}{R_{pf}} + \beta E(t) \quad (2)$$

$$C_f \left\{ \frac{\partial T_f}{\partial t}(x,t) + \bar{u} \frac{\partial T_f(x,t)}{\partial x} \right\} = \frac{T_p(x,t) - T_f(x,t)}{R_{pf}}. \quad (3)$$

Figure 1 shows the corresponding network.

Several approximations are made in this model. The heat losses at the back side and the edges of the collector are neglected by the assumption of a perfect insulation. Also neglected is the radiation absorbed by the cover plate. The temperatures depend on one variable of space defined in the direction of the fluid flow.

The capacities and the heat resistances as well as the fluid flow velocity, are assumed to be constant. If sufficient boundary and initial conditions are known, the collector temperatures can be solved from (1)–(3). In practical testing, only the fluid inlet and outlet temperature are easy to measure. These two conditions do not suffice to define completely the differential problem (1)–(3).

NOMENCLATURE

A, B, M, K	functions, used as abbreviations for various relations
c	specific heat of water [J kg^{-1} K^{-1}]
C	heat capacity per m^2 [J K^{-1} m^{-2}]
E	the insolation [W m^{-2}]
$\hat{E}$	the Fourier transform of E [W m^{-2} s]
E_0	constant, defining the imaginary insolation (13) [W m^{-2}]
L	length of the collector in the flow direction [m]
$\dot{m}$	mass flow rate per m^2 [kg s^{-1} m^{-2}]
R	thermal resistance per m^2 [W^{-1} K m^2]
R_L	total heat loss resistance per m^2 [W^{-1} K m^2]
t	coordinate of time [s]
t_e	time interval of the measurements [s]
t_0	initial time of the measurements [s]
t_p	period of the varying imaginary insolation (13) [s]
T	the temperature of a part of the collector [K]
$\hat{T}$	the Fourier transform of T [K s]
$\bar{u}$	velocity of the fluid flow [m s^{-1}]
x	space coordinate in the flow direction [m]
$\tilde{X}(\omega)$	the Fourier transform of the insolation [J m^{-2}]
X_R, X_I	real and imaginary part of the complex function $\tilde{X}(\omega)$ [J m^{-2}]
$\tilde{Y}(\omega)$	the Fourier transform of the difference of the fluid inlet temperature and the ambient temperature [K s]
Y_R, Y_I	real and imaginary part of the complex function $\tilde{Y}(\omega)$ [K s]
$\tilde{Z}(\omega)$	generalized expression of the useful energy [J m^{-2}]
Z_R, Z_I	real and imaginary part of the complex function $\tilde{Z}(\omega)$ [J m^{-2}].

Greek symbols

β	absorptance–transmittance product
δ, η	coordinates of the Cartesian coordinate system defining the points $(Y_R/X_R, Z_R/X_R)$ or $(Y_I/X_I, Z_I/X_I)$, Fig. 2 [W m^{-2} K^{-1}, —]
ΔE_0	constant, defining the imaginary insolation (13) [W m^{-2}]
Δt	interval between two successive moments of measurement [s]
ω	Fourier variable [s^{-1}].

Subscripts

a	ambient
f	fluid
g	cover plate
p	absorber plate.

Fortunately, the type of collectors considered has the representative property that both the heat resistances R_{ag} and R_{pf} are much smaller than R_{pg}. Moreover, it is assumed that R_{pg} can be approximated by the heat loss resistance R_L. In the following, the ratios of R_{ag}/R_L and R_{pf}/R_L are neglected with respect to one.

In this case it is possible to find an approximate solution of (1)–(3). Not only can the calculations be simplified, but the measurements of the fluid inlet and outlet temperatures are sufficient to find approximations of the temperatures within the collector [3].

Insight in the dynamic behaviour of the collector can be obtained by studying the various temperatures in the frequency domain. They follow from the Fourier transform of the time dependent set of differential equations (1)–(3).

Introducing the finite Fourier transform of the temperature, thus

$$\hat{T}(x,\omega) = \int_0^{t_e} e^{-i\omega t}\, T(x,t)\, dt, \tag{4}$$

and, analogously, for the other time-dependent

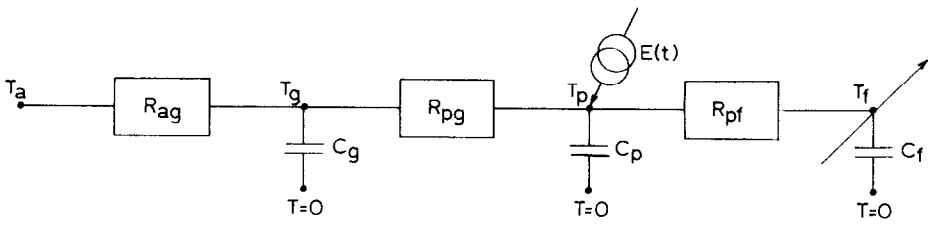

FIG. 1. The heat resistance network of the collector model.

quantities, the set of equations (1)–(3) can be transformed into the frequency domain.

It is well-known (see [4]), the differential behaviour with respect to the time variable t transforming into an algebraic one with respect to the Fourier variable ω, in these equations.

Eliminating $\hat{T}_g(x,\omega)$ and $\hat{T}_p(x,\omega)$, the transformed set of (1)–(3) reduces to a first-order ordinary differential equation of $\hat{T}_f(x,\omega)$ with respect to the space variable x. Direct integration results in the approximate fluid temperature $\hat{T}_f(x,\omega)$, expressed as functions of the measured weather variables, the insolation $\hat{E}(\omega)$ and the ambient temperature $\hat{T}_a(\omega)$ and the measurements of the fluid inlet and outlet temperatures, $\hat{T}_f(0,\omega)$ and $\hat{T}_f(L,\omega)$, respectively. Of course, this expression contains the heat resistances and heat capacities occurring in (1)–(3) as parameters (see Appendix).

Analogous to the methods for steady conditions, the collector test method for transient weather conditions treated in this paper, compares the useful energy with the input parameters such as the solar radiation, the ambient temperature and the fluid inlet temperature.

A relation between these quantities is found by writing out the difference of the fluid inlet and outlet temperature, $\hat{T}_f(L,\omega)-\hat{T}_f(0,\omega)$, being a factor of the useful energy, using the approximate fluid temperature $\hat{T}_f(x,\omega)$.

Rearranging some terms, the basic relation of our test method can be derived (see Appendix), yielding

$$\tilde{Z}(\omega)=\beta\tilde{X}(\omega)-\tilde{Y}(\omega)/R_L. \tag{5}$$

In two ways, (5) can be considered as a generalization of the classical Hottel–Whillier–Bliss equation for steady conditions. The functions $\tilde{X}(\omega)$, $\tilde{Y}(\omega)/R_L$ and $\tilde{Z}(\omega)$ have to be understood as generalized forms of, respectively, the insolation, the heat losses and the useful energy. Their main parts consist of the corresponding contributions in the frequency domain, computed with the aid of the direct measurements obtained during the time interval t_e. Additional contributions follow from the effects of the thermal capacities during transient conditions. Secondly, with respect to the HWB equation, the meaning of relation (5) has been extended from $\omega=0$ to any value of ω in the frequency domain. This means that for instance an integral representing a simple integration in the time domain over the interval t_e, has been replaced by a corresponding Fourier transform of the type (4).

The functions $\tilde{X}(\omega)$, $\tilde{Y}(\omega)$ and $\tilde{Z}(\omega)$ are complex functions each having a real and an imaginary part. Therefore, (5) can equivalently be written as

$$Z_R(\omega)=\beta X_R(\omega)-Y_R(\omega)/R_L \tag{6}$$

$$Z_I(\omega)=\beta X_I(\omega)-Y_I(\omega)/R_L. \tag{7}$$

The collector test method is based on (6) and (7). At a given flow rate, $\dot{m}c$, experimental measurements are made of the insolation, the ambient temperature and fluid inlet and outlet temperature, respectively. These measurements are necessary to compute the values of the real functions X_R, X_I, Y_R, Y_I, Z_R and Z_I for the time interval t_e (cf. Appendix). As explained in the Appendix, the relations (6) and (7) have been arranged in such a way that X_R, X_I, Y_R and Y_I are independent of β and $1/R_L$ and the dependence of Z_R and Z_I on both parameters is very weak. Moreover, the most important capacity of Z_R and Z_I turns out to be C_p+C_f, while the influences of respectively C_gR_{ag} on Y_R and Y_I and C_pR_{pf} on Z_R and Z_I are very small. Usually, reasonable estimates of the resistances and capacities can be obtained from the collector design. Using these estimates, numerical values of the functions in (6) and (7) can be computed for each choice of the Fourier variable ω.

Each value of ω leads to two linear equations in the characteristic collector parameters β and $1/R_L$. In principle, these parameters can be determined by a least-square method if a sufficient number of different equations can be obtained by particular choices of ω.

An alternative representation of (6) and (7), more convenient for a direct and clear illustration, is given by the equations

$$Z_R(\omega)/X_R(\omega)=\beta-[Y_R(\omega)/X_R(\omega)]/R_L \tag{8}$$

$$Z_I(\omega)/X_I(\omega)=\beta-[Y_I(\omega)/X_I(\omega)]/R_L. \tag{9}$$

In this case the points $(Y_R/X_R, Z_R/X_R)$ and $(Y_I/X_I, Z_I/X_I)$ can be plotted in a two dimensional Cartesian coordinate system (δ,η). In the case of a sufficient number of different points, a straight line can be defined as a least-square approximation according to (8) and (9). The collector characteristics β and $1/R_L$ are defined by the intersection of the line with the η-axis and the slope of the line (see Fig. 2). Particularly, in the case of a fixed inlet temperature giving nearly constant heat losses, and a varying insolation, it can intuitively be expected that the functions $\tilde{Y}(\omega)$ and $\tilde{X}(\omega)$ show a different behaviour as functions of ω. Whether the corresponding points in the (δ,η)-plane with abscissas $\delta=Y_R/X_R$ and $\delta=Y_I/X_I$, respectively, will show sufficiently different positions in the (δ,η)-plane, partly depends on the choices of ω with respect to the dominant frequencies of the insolation.

A last remark concerns the transient weather characteristics of the insolation. Due to passing clouds the dominant periods of the insolation turn out to be relatively large. In our test method we allowed for realistic periods of say 600–1200 s found from our own experiments as well as from literature [5].

4. EXPERIMENTAL APPARATUS AND PRACTICAL APPLICATION OF THE TEST METHOD

As illustrated by the photograph in Fig. 3, the collector considered was tested on a movable frame work placed outdoors. The collector is a part of a closed loop, partly consisting of copper pipes. An ordinary central-heater pump (Grundfoss) circulates the water with a constant mass flow. The circulating fluid enters the collector with a constant inlet temperature. During

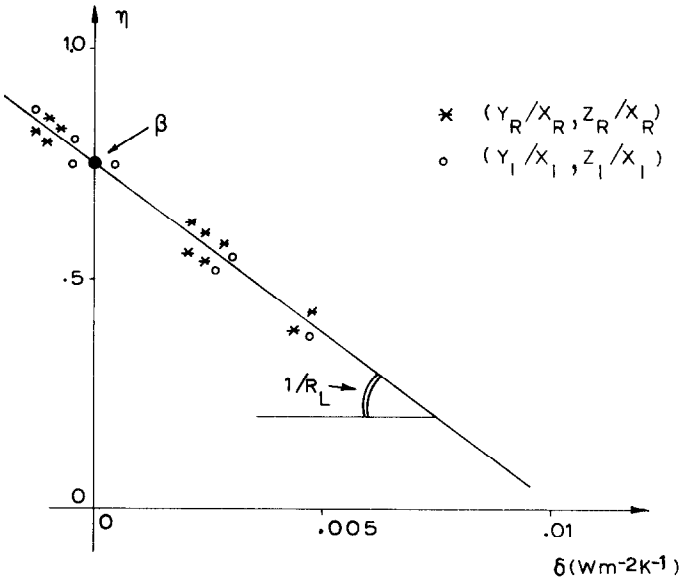

FIG. 2. The collector parameters β and $1/R_L$ defined by a least-square approximation.

its passage through the collector, the fluid is heated by the solar radiation. After the outlet temperature has been registered, the fluid is cooled to the inlet temperature. A heat exchanger connected with the tap water, causes a temperature drop to a value of approx. 1 K below the inlet temperature. Next, a fine adjustment of the (constant) inlet temperature is obtained by means of electric heating.

This test method requires a transient insolation. In the case of a (nearly) constant solar radiation, sufficient fluctuations can be artificially obtained by periodically covering the collector with a semi-transparent shield.

During the experiments, the collector was kept manually oriented perpendicular to the direction of the sun.

Data of the insolation, the inlet and the outlet

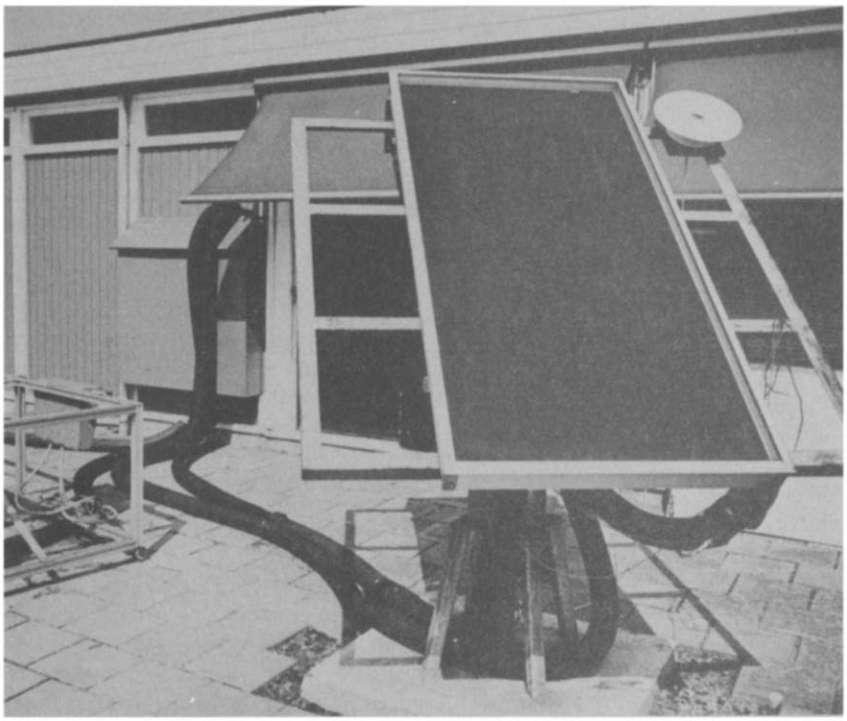

FIG. 3. The collector to be tested outside.

temperature, the fluid mass flow and the ambient temperature are periodically measured at discrete time intervals of 10 s during the period of the experiment. A data logger records these data on tape to be used for computer calculations afterwards. Examples of the results of the recorded series of measurements are shown in the Figs. 4(a) and (b). Figure 4(a) illustrates a varying insolation caused by passing clouds. Figure 4(b) shows, that during a stationary insolation the transient behaviour can be obtained by a periodical covering of the collector by a shield.

In practice, the test method is applied to data obtained during a time interval $(0, t_e)$ being a part of the complete series of experimental measurements.

These data are used for the numerical determination of the functions $\tilde{X}$, $\tilde{Y}$ and $\tilde{Z}$, required for the application of the test method.

5. A NUMERICAL EXPERIMENT FOR THE COLLECTOR TEST METHOD

In order to verify its validity the test method has been applied to numerical data obtained from an imaginary flat plate collector operated under imaginary transient weather conditions. A model of a simple collector, of which the properties can be calculated analytically follows from (1)–(3) with the particular choices of $R_{ag} = 0$ and $R_{pf} = 0$. In fact, this model represents an ideal collector with an excellent heat transfer between the absorber and the fluid, perfectly insulated at the backside, situated in a windy climate.

In this case, the fluid temperature can be described by the one-node model

$$(C_p + C_f)\frac{\partial T_f}{\partial t} + C_f \bar{u}\frac{\partial T_f}{\partial x} + \frac{T_f}{R_L} = \beta E(t) + T_a/R_L. \quad (10)$$

The solution of (10) satisfying a constant fluid inlet temperature, yields an analytic expression of the fluid outlet temperature, namely

$$T_f(L,t) = T_f\left(0, t - \frac{C_p + C_f}{\dot{m}c}\right)\exp\left[-(\dot{m}cR_L)^{-1}\right] + \int_0^{(C_p+C_f)/\dot{m}c} \frac{\exp\left[-k/R_L(C_p+C_f)\right]}{C_p + C_f} \times \left\{\beta E(t-k) + \frac{T_a(t-k)}{R_L}\right\} dk, \quad (11)$$

in which

$$\dot{m}c = C_f \bar{u}/L. \quad (12)$$

Furthermore, a constant ambient temperature and a periodically varying insolation,

$$E(t) = E_0 + \Delta E_0 \operatorname{sign}(\sin 2\pi t/t_p), \quad t \geqslant 0 \quad (13)$$

are assumed. For the imaginary collector, simulated numerical expressions corresponding with the required experimental measurements can be obtained from (11) and (13) at selected intervals after supplying representative numerical data of the insolation, the ambient temperature, the fluid inlet temperature and the known collector parameters. The following representative data are assumed:

$$\begin{aligned} \beta &= 0.80 \\ C_p &= 3600 \text{ J K}^{-1} \text{ m}^{-2} \\ \dot{m}c &= 150 \text{ W K}^{-1} \text{ m}^{-2} \\ E_0 &= 600 \text{ W m}^{-2} \\ t_p &= 1200 \text{ s} \\ \Delta t &= 10 \text{ s} \\ R_L &= 0.16 \text{ K W}^{-1} \text{ m}^2 \\ C_f &= 6750 \text{ J K}^{-1} \text{ m}^{-2} \\ T_f(0,t) &= 40°\text{C} \\ \Delta E_0 &= 300 \text{ W m}^{-2} \\ T_a &= 20°\text{C}. \end{aligned} \quad (14)$$

Particularly, it is noted that t_p has been chosen in the range of the dominant periods of varying insolation. With the aid of these data, the simulated expressions can be computed. Our test method has been applied to several series of data obtained for various choices of the time interval t_e. As a typical example, we show the results obtained for a time interval of $t_e = 2100$ s, beginning at $t_0 = 1200$ s using the insolation (13). The numerical values of X_R, Y_R and Z_R as functions of the Fourier variable are shown in Fig. 5(a). They are influenced by numerical errors, since only the values of the integrand are available at discrete time intervals of 10 s for the computation of the integrals by a standard integration procedure from a computer software library.

The size of the errors can be obtained by comparing the values of X_R, Y_R and Z_R in Fig. 5(a) with those of the corresponding analytic expressions. For instance, the values of $X_R(\omega)$ in Fig. 5(a) can be compared with the results of the analytic integration of the expression

$$X_R(\omega) = \int_{t_0}^{t_0+t_e} \cos \omega t \{E_0 + \Delta E_0 \times \sin[2\pi(t-t_0)/t_p]\}\, dt. \quad (15)$$

A plot of $\Delta X_R/X_R$ in Fig. 5(a) shows an increasing relative error for values of ω when X_R becomes zero.

The representation of the points $(Y_R/X_R, Z_R/X_R)$ in the (δ, η)-plane corresponding with (8) and (9) is given in Fig. 5(b). The same serial number is given to points with the same value of ω in both Figs. 5(a) and (b). Also drawn in Fig. 5(b) is the line defined by $\beta = 0.80$ and $R_L = 0.16$. The theoretical least-square approximation of the points has to coincide with this line. Analysing Figs. 5(a) and (b), the following can be noticed:

(i) Points in Fig. 5(b) corresponding with values of ω where X_R, Y_R and Z_R have values near extrema in Fig. 5(a), such as in the points with serial number 1–7, 12–14, 18–23, are reasonably situated near the theoretical line.

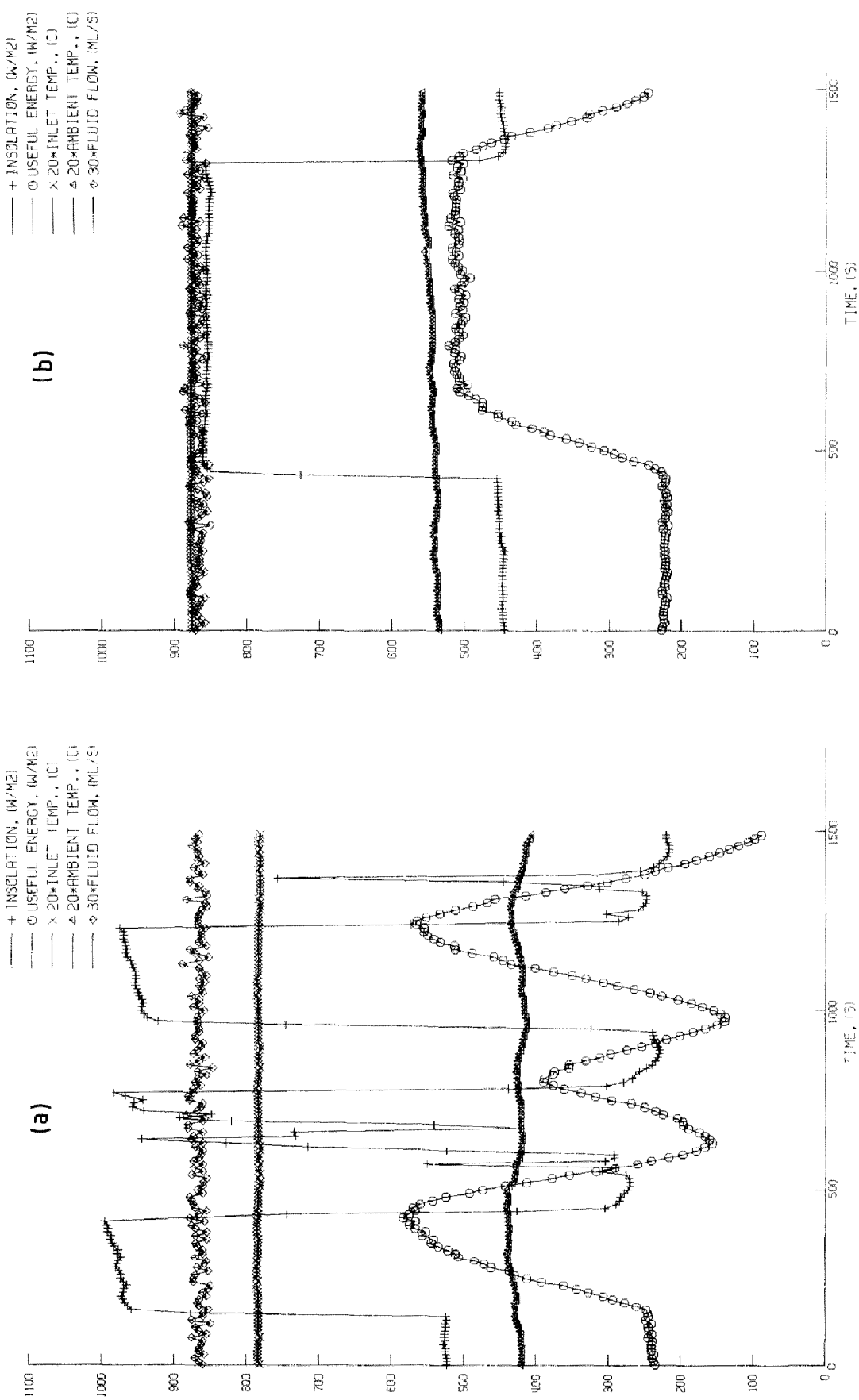

FIG. 4. The transient behaviour of the insolation, the useful energy and the ambient temperature in (a) the case of a natural varying solar radiation and (b) the case of a periodic shielding.

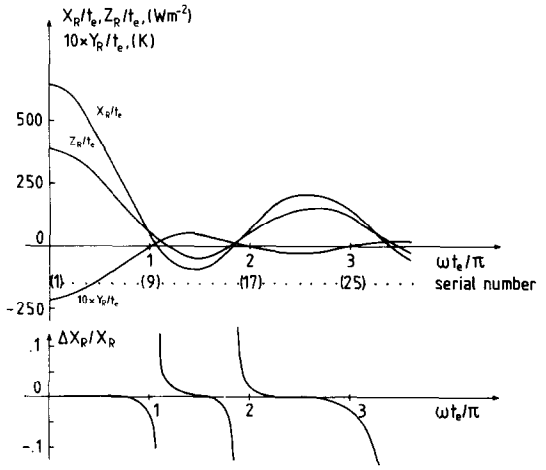

FIG. 5(a). The dependence of X_R, Y_R and Z_R on the Fourier variable ω. Also shown is the relative numerical error $\Delta X_R/X_R$.

(ii) Points with a number near 9, 16 or 28, corresponding with values of ω where X_R, Y_R and Z_R in Fig. 5(a), are near zero, show more deviations from this line (16 and 28 are outside the frame of the figure). In these regions, both X_R, Y_R and Z_R and its relative errors are fast varying with respect to ω.

(iii) Of particular importance for the application of the least square approximation are points in Fig. 5(b) situated near the η-axis with a small value of $\delta = Y_R/X_R$. They follow for values of ω, where $Y_R(\omega)$ is near zero in Fig. 5(a), such as the numbers 9, 16 and 26. Unfortunately they are situated in a region with a large sensitivity for errors, described in (ii).

The properties of X_I, Y_I and Z_I are represented in Figs. 6(a) and (b) analogously to those of X_R, Y_R and Z_R in Figs. 5(a) and (b).

(iv) Similarly to note (i), points with numbers 2–13, 22–29 in Fig. 6(b), resulting from values of ω round extrema in Fig. 6(a) are near the theoretical line.

(v) Points such as 14–16, 18–20 are sensitive of errors by reasons given in note (ii).

(vi) Near $\omega t_e/\pi \approx 2$, the function $Y_I(\omega)$ has a minimum value near zero in Fig. 6(a), which implies a stable behaviour of Y_I with respect to ω. In the case that for the same value of ω, $X_I(\omega)$ has a sufficiently large absolute value, a corresponding point near both the η-axis and the theoretical line of Fig. 6(b) can be obtained. The point with number 17 in Fig. 6(b) satisfies this condition. It has been found that the value of $X_I(\omega)$ at the minimum value of $Y_I(\omega)$ near $\omega t_e/\pi \approx 2$, strongly depends on the time interval t_e, or what is the same, in fact, on the ratio of t_e and t_p, the period of the varying insolation (13). The dependence is illustrated in Fig. 7, resulting from calculations with the imaginary collector model starting with $t_0 = 1200$ s and various values of t_e. Relatively large values of X_I are found near the extrema at $t_0 + t_e = 3300$ s and $t_0 + t_e = 3900$ s. Hence, appropriate points near the theoretical line in Fig. 6(b) are found for the intervals 1200–3300 s and 1200–3900 s. On the other hand, the position of the point for 1200–3000 s, yielding a vanishing value of X_I (Fig. 7), is unstable.

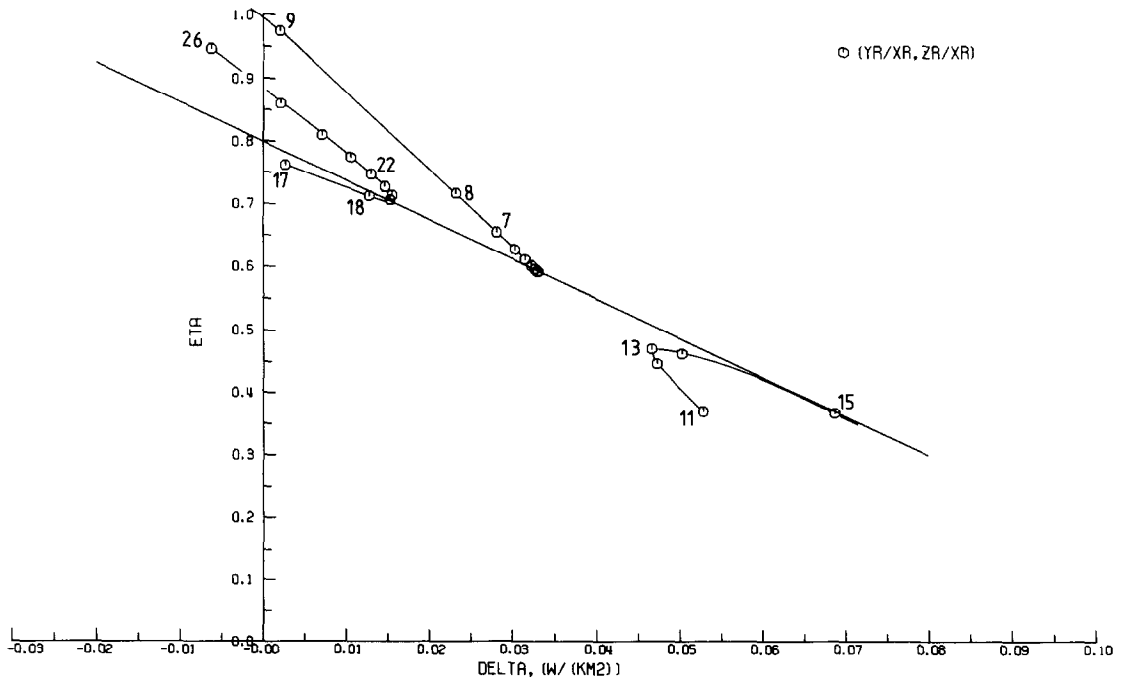

FIG. 5(b). A plot of points $(Y_R/X_R, Z_R/X_R)$ corresponding with discrete equidistant values of ω from Fig. 5(a). Theoretically, the points have to coincide with the drawn line.

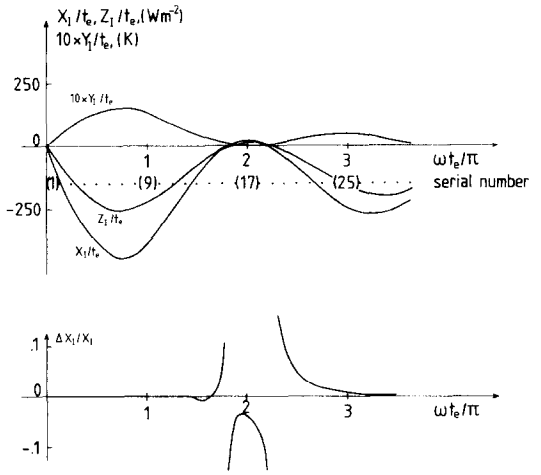

FIG. 6(a). The dependence of X_I, Y_I and Z_I on the Fourier variable ω. Also shown is the relative numerical error $\Delta X_I/X_I$.

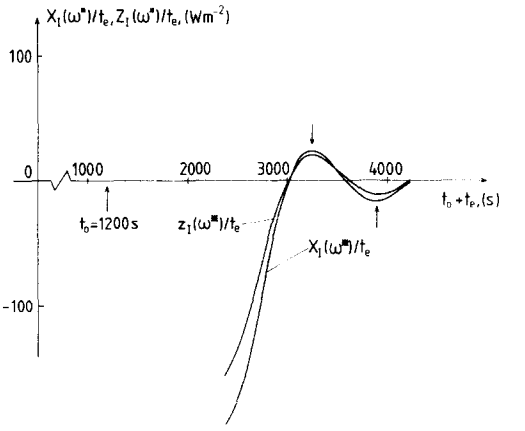

FIG. 7. The values of X_I and Z_I for the Fourier variable ω^*, where Y_I has an extremum near $\omega t_e/\pi \approx 2$ for a variable time interval, t_e.

6. APPLICATION OF THE TEST METHOD

The test method has been applied to a commercially available conventional flat plate solar collector (RENOR, type MP, collector produced by EBS, Grave, The Netherlands). This collector can be represented by the mathematical model of Section 2. A sketch is given in Fig. 8. Placed on the test installation outside, the collector operates under actual weather conditions. If necessary, the transient behaviour of the insolation is intensified by a periodical shielding of the collector. The fluid inlet temperature and the fluid flow rate are adjusted to fixed values.

During periods of 7200–9000 s the insolation, the ambient temperature, the fluid inlet and outlet temperature and the fluid flow have been measured every 10 s. Parts of series of such measurements are already given in Figs. 4(a) and (b), respectively. The experimental data are used to test the method. After choosing an initial time t_0, a time interval t_e and reasonable estimates of the heat capacities and heat resistances, the properties of X_R, Y_R, Z_R and X_I, Y_I, Z_I, respectively, can be determined as functions of ω.

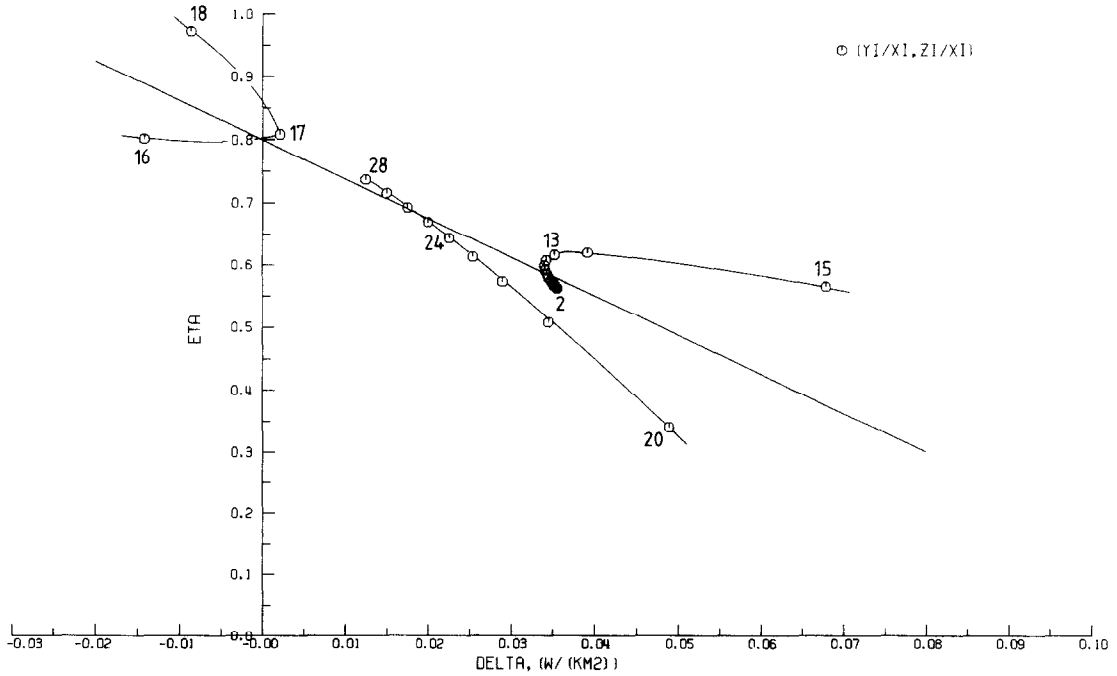

FIG. 6(b). A plot of points $(Y_I/X_I, Z_I/X_I)$ corresponding with discrete equidistant values of ω from Fig. 6(a). Theoretically, the points have to coincide with the drawn line.

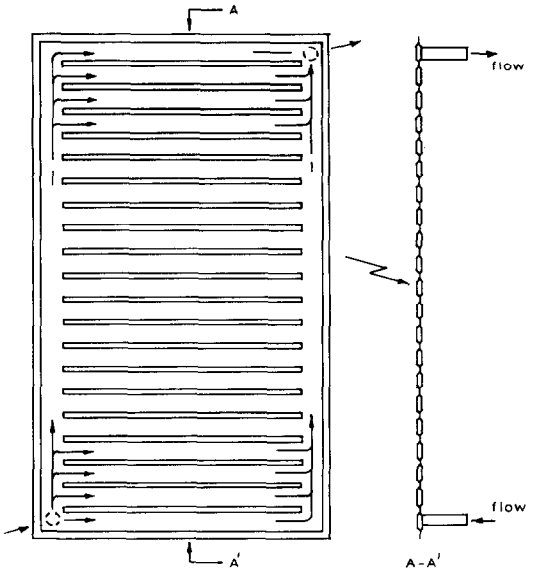

FIG. 8. A sketch of the conventional collector.

Because of the dominant low frequencies of the insolation shown in Figs. 4(a) and (b), a behaviour analogous to that of Figs. 5(a) and 6(a), respectively, is found. The representation of the corresponding points in the (δ, η)-plane similar to Figs. 5(b) and 6(b), yields disappointing results. Because of very large variations in the positions of the points, a consistent least-square approximation is not possible, in many cases. Clearly, several kinds of error influence the results. Firstly, there are the numerical errors already mentioned in Section 5 and the errors caused by the approximation of the collector by the simple mathematical model. The instruments of the testing apparatus, such as the solarimeter, cause a second type of error.

In fact, reliable points are obtained only from values of ω near the first extrema of X_R, Y_R, Z_R defined by $0 \leqslant \omega t_e/\pi < 0.6$ and the first extrema of X_I, Y_I, Z_I defined by $0.25 < \omega t_e/\pi < 1.25$. In both cases, there results a small string of points in the (δ, η)-plane, very near to that of $\omega = 0$ in the case of X_R, Y_R, Z_R. Points corresponding with different values of ω, generally showing an unpredictable and erroneous position, cannot be used for the application of a least-square approximation. There is only one exception, namely the case already mentioned in Section 5 (vi). If the stable minimum value of $Y_I(\omega)$ near $\omega t_e/\pi \approx 2$, is combined with a sufficiently large absolute value of $X_I(\omega)$, for the same ω, a well-defined point near the η-axis in the (δ, η)-plane can be found.

To this end, the values of X_I for this particular value of ω are determined by varying the time interval t_e for a fixed initial time t_0, similarly to Fig. 7. Well-defined points in the (δ, η)-plane are obtained from time intervals defined by t_0 and values of t_e selected at not too small extrema of X_I. A typical example obtained from a series of experimental measurements is shown in Fig. 9. In this case, the time intervals of 2000–4700 s and 2000–6500 s yield points near the η-axis in the (δ, η)-plane, which can be used for the least-square approximation.

For each single time interval, the test method can be applied to a limited selection of values of ω. Generally, this number is too small and there is too much spread in the position of some points to determine reliable values of the collector characteristics by a least-square method. Taking different time intervals from the same series of measurements, a superposition of convenient points in the (δ, η)-plane can be derived.

Firstly, a cluster of strings resulting from X_R, Y_R, Z_R and X_I, Y_I, Z_I, respectively, near the point corresponding with $\omega = 0$, is found. In the case of experimental measurements with a fixed inlet temperature defining nearly constant heat losses of the collector, these strings constitute a cloud of points at a nearly fixed position in the (δ, η)-plane. An extension of points situated near the η-axis in the (δ, η)-plane is obtained by considering the functions X_I, Y_I, Z_I for selected time intervals t_e and particular values of ω, as described. Figure 10 shows the results for 27 time intervals taken from one series of experimental measurements with a fixed inlet temperature. For each time interval, the points with values of $\omega = 0$ for X_R, Y_R,

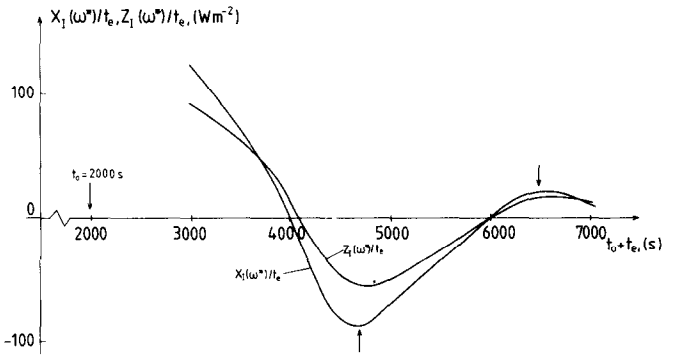

FIG. 9. The values of $X_I(\omega^*)$ and $Z_I(\omega^*)$ for a variable time interval, ω^* determined by the stable $Y_I(\omega^*)$ near $\omega t_e/\pi \approx 2$.

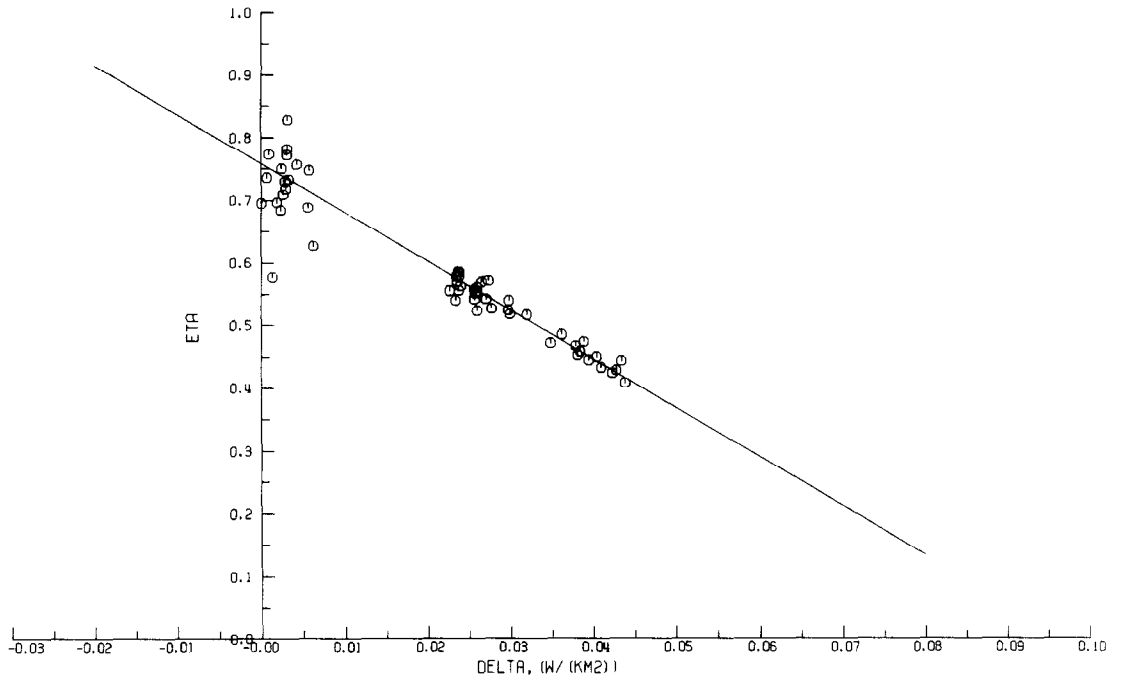

FIG. 10. A plot of points resulting from one series of experimental measurements with a fixed inlet temperature. The straight line defines the collector parameters.

Z_R and $\omega t_e/\pi = 0.75$ for X_I, Y_I, Z_I are expressed. (Compare the extrema in Figs. 5(a) and 6(a).) At the same time are shown the points with a value of ω, where $Y_I(\omega)$ has a minimum near $\omega t_e/\pi \approx 2$. Also drawn is the straight line as a least-square approximation defining the collector characteristics of $\beta = 0.755 \pm 0.017$ and $R_L = 7.39 \pm 0.70$ K W^{-1} m^2. A verification of the results of the collector characteristics can be obtained if experimental measurements can be made for different fluid inlet temperatures. Corresponding clouds of points, resulting for values of ω near zero, are found at different positions in the (δ, η)-plane. In the case of a

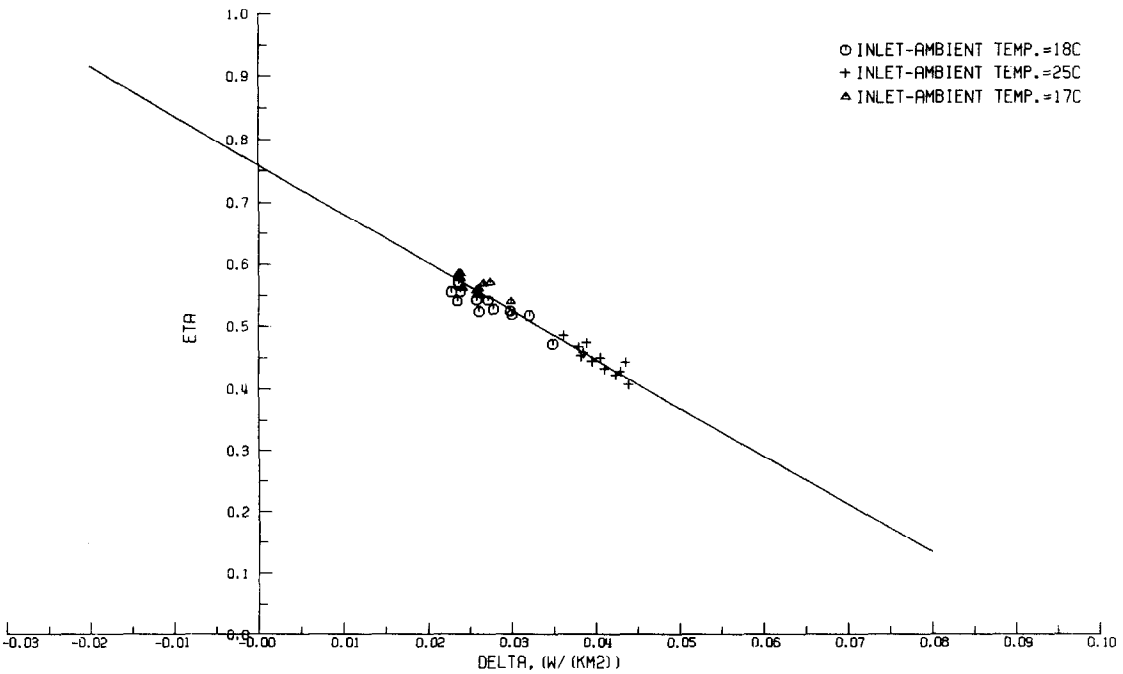

FIG. 11. A plot of points from series of experimental measurements with different fluid inlet temperatures.

sufficient spread, they can define a straight line as a least-square approximation.

Figure 11 shows the clouds of points for six time intervals taken from three experimental measurements each with a different fluid inlet temperature. The points with $\omega = 0$ for X_R, Y_R, Z_R and $\omega t_e/\pi = 0.75$ for X_I, Y_I, Z_I are taken for each time interval. The characteristics are found to be $\beta = 0.759 \pm 0.010$ and $R_L = 7.82 \pm 0.34$ K W^{-1} m^2, in this case.

It will be clear that the best results can be obtained in the case that measurements with sufficiently different inlet temperatures are available.

7. CONCLUSIONS

This paper describes an outdoor collector test method appropriate for transient weather conditions.

Instead of an expensive solar simulator, the actual sunlight supplies the radiation of the collector.

The collector characteristics β and R_L are obtained by a least-square method from a set of algebraic equations, relating the generalized functions of the insolation, the heat losses and the useful energy, respectively. These equations are derived by applying the Fourier transformation with respect to a finite time interval t_e to the time-dependent equations representing the collector model. Because of various kinds of errors, a limited range of values of ω leads to an appropriate equation.

The results of the collector characteristics obtained from various separate time intervals t_e show a relatively large spread.

A superposition of points obtained from several time intervals chosen from a series of experimental measurements with a fixed fluid inlet temperature yields better results. In this case, the least-square approximation is comparable with results obtained by other methods.

The best results follow from the application of the method for values of ω near zero to time intervals taken from experimental data measured with different inlet temperatures.

REFERENCES

1. R. Posorski, K. Massmeyer, R. Schröer and H. J. Stein, Experimental experience with standards for solar collector testing, *Proc. ISES Solar World Forum*, Brighton, pp. 1520–1525. Pergamon Press, Oxford (1982).
2. B. A. Rogers, A method of collector testing under transient conditions, *Proc. ISES Solar World Forum*, Brighton, pp. 898–902. Pergamon Press, Oxford (1982).
3. W. Kamminga, The approximate temperatures within a flat plate solar collector under transient conditions, *Int. J. Heat Mass Transfer* **28**, 433–440 (1985).
4. R. V. Churchill, *Operational Mathematics*. McGraw-Hill, New York (1958).
5. A. Saito, Y. Utaka, T. Tsuchio and K. Katayama, Transient response of flat plate solar collector for periodic solar intensity variation, *Sol. Energy* **32**, 17–23 (1984).

APPENDIX: THE DERIVATION OF THE GENERALIZED FUNCTIONS $\hat{X}(\omega)$, $\hat{Y}(\omega)$ AND $\hat{Z}(\omega)$

Using Fourier transforms of the type (4) applied to the differential equations (1)–(3), the ordinary differential equation for $\hat{T}_f(x, \omega)$ follows by straightforward calculation, namely

$$A(\omega)\hat{T}_f(x,\omega) + B(\omega)\frac{\partial \hat{T}_f}{\partial x}(x,\omega) = M(\omega) + K(x,\omega), \quad \text{(A1)}$$

in which

$$A(\omega) = 1/R_L + i\omega C_f[(C_p + C_f)/C_f + i\omega C_p R_{pf}] \quad \text{(A2)}$$

$$B(\omega) = C_f\bar{u}(1 + i\omega C_p R_{pf}) \quad \text{(A3)}$$

$$M(\omega) = \beta\hat{E}(\omega) + \hat{T}_a(\omega)/[R_L(1 + i\omega C_g R_{ag})] \quad \text{(A4)}$$

$$K(x,\omega) = -C_f(1 + i\omega C_p R_{pf})[e^{-i\omega t_e} T_f(x,t_e) - T_f(x,0)] - C_p[e^{-i\omega t_e} T_p(x,t_e) - T_p(x,0)] - \frac{C_g R_{ag}}{R_L(1 + i\omega C_g R_{ag})} \times [e^{-i\omega t_e} T_f(x,t_e) - T_f(x,0)]. \quad \text{(A5)}$$

The solution of $\hat{T}_f(x, \omega)$ follows by direct integration of (A1) with respect to the space variable x. The resulting expression of $\hat{T}_f(x, \omega)$, not given here, is used to define the basic relation of the test method, being the useful energy proportional with

$$\hat{T}_f(L,\omega) - \hat{T}_f(0,\omega) = (1 - e^{-AL/B})[M/A - \hat{T}_f(0,\omega)] + \frac{1}{B}\int_0^L K(v,\omega)\, e^{-A(L-v)/B}\, dv. \quad \text{(A6)}$$

With some calculation and using the approximations $R_{pf} \ll R_L$ and $R_{ag} \ll R_L$, (A6) can be written in the alternative form of the basic equation (5). Defining

$$\hat{X}(\omega) = \hat{E} \quad \text{(A7)}$$

$$\hat{Y}(\omega) = \frac{\hat{T}_f(0,\omega) + \hat{T}_f(L,\omega)}{2} - \hat{T}_a + \frac{C_g R_{ag}}{1 + i\omega C_g R_{ag}} \times [\hat{T}_a\, i\omega + e^{-i\omega t_e} T_a(t_e) - T_a(0)], \quad \text{(A8)}$$

the generalized form of the useful energy can be written as

$$\hat{Z}(\omega) = \left(\frac{A}{1 - e^{-AL/B}} - \frac{1}{2R_L}\right)[\hat{T}_f(L,\omega) - \hat{T}_f(0,\omega)] + (A - 1/R_L)\hat{T}_f(0,\omega) + \frac{AC_f/B}{1 - e^{-AL/B}} \times [(C_p + C_f)/C_f + i\omega C_p R_{pf}] \int_0^L e^{-A(L-v)B} \times \{e^{-i\omega t_e} T_f(v,t_e) - T_f(v,0)\}\, dv. \quad \text{(A9)}$$

The last integral of the RHS of (A9) represents the capacitive heat stored within the collector at $t = 0$ and $t = t_e$, respectively. The fluid temperature T_f within the collector occurring in the integrand of this integral can be approximated using the measured fluid outlet temperature $T_f(L, t)$ during a certain time interval [3].

Obviously, $\hat{X}$ and $\hat{Y}$ are independent of β and $1/R_L$. The dependence of $Z(\omega)$ on both parameters can be shown to be very weak. For instance, $1/R_L$ is a term of A occurring in some factors of the terms of (A9). Series expansions of this factors show the higher order terms of $1/R_L$ to vanish, in most cases.

The influence of the other unknown heat resistances and capacities will be shortly discussed. The last term of (A8) is equal to zero for a constant ambient temperature. In practice, the ambient temperature having only small variations during one period of experimental measurements, the influence of $C_g R_{ag}$ can be neglected in $\hat{Y}(\omega)$.

As discussed in Section 6 the values of ω applied in the test method are limited and are small ($\omega t_e/\pi \leqslant 2$). The term $i\omega C_p R_{pf}$ occurring in the expressions $(C_p + C_f)/C_f + i\omega C_p R_{pf}$ and $1 + i\omega C_p R_{pf}$ is small with respect to $(C_p + C_f)/C_f$ and 1, respectively. These expressions are present in $\tilde{Z}(\omega)$, partly in the factors A and B of $\tilde{Z}(\omega)$, (A9). This implies that $\tilde{Z}(\omega)$ hardly depends on $C_p R_{pf}$ for most values of ω. After some calculation and using series expansions of some exponentials of $\tilde{Z}(\omega)$, $C_p + C_f$ is found to be the main capacity in (A9). Usually, estimates of the heat capacities can be obtained from the collector design.

The real functions $X_R(\omega)$, $X_I(\omega)$, $Y_R(\omega)$, $Y_I(\omega)$, $Z_R(\omega)$, $Z_I(\omega)$ are defined as the real and the imaginary part of respectively the complex functions $\tilde{X}(\omega)$, $\tilde{Y}(\omega)$ and $\tilde{Z}(\omega)$.

METHODE D'EXPERIMENTATION D'UN COLLECTEUR SOLAIRE AVEC UTILISATION DES FONCTIONS DE TRANSFERT DE FOURIER

Résumé—On développe un méthode d'essai des collecteurs essentiellement basée sur des conditions variables dans le temps. Une transformation de Fourier des équations différentielles décrivant le collecteur conduit à des relations pour les caractéristiques du collecteur. A cause des erreurs, seul un nombre limité de ces équations, défini par des choix particuliers à la fois de l'intervalle de temps t_e et de la variable de Fourier ω, peut être appliqué dans la méthode d'essai. Les paramètres du collecteur peuvent être déterminés par une méthode des moindres carrés qui utilise une série d'expériences faites avec une température de fluide fixée à l'entrée. Les résultats sont comparables avec ceux obtenus à partir d'un plus grand nombre de séries de mesures avec différentes valeurs de la température d'entrée du fluide.

ERFAHRUNGEN MIT EINER TESTMETHODE FÜR SOLARKOLLEKTOREN, DIE FOURIER-TRANSFORMATIONEN ANWENDET

Zusammenfassung—Es wurde eine Testmethode für Kollektoren entwickelt, die im wesentlichen auf zeitlich veränderlichen Bedingungen basiert. Eine finite Fourier-Transformation der den Kollektor beschreibenden Differentialgleichungen führt zu Beziehungen, die den Kollektor charakterisieren. Wegen der Fehler kann nur eine begrenzte Anzahl dieser Gleichungen, welche durch eine besondere Auswahl von Zeitintervall t_e und Fourier Variabler ω definiert sind, in der Testmethode angewandt werden. Die Kollektorparameter werden nach der Methode der kleinsten Fehlerquadrate bestimmt, wobei nur Serien von Messungen mit gleicher Fluideintrittstemperatur verwendet werden. Die Ergebnisse sind vergleichbar mit jenen, die aus mehreren Serien von Messungen bei unterschiedlichen Fluideintrittstemperaturen ermittelt werden.

РЕЗУЛЬТАТЫ ЭКСПЕРИМЕНТАЛЬНОГО МЕТОДА ИССЛЕДОВАНИЯ СОЛНЕЧНОГО КОЛЛЕКТОРА С ИСПОЛЬЗОВАНИЕМ ФУНКЦИЙ ФУРЬЕ-ПРЕОБРАЗОВАНИЯ

Аннотация—Предложен экспериментальный метод нестационарного исследования коллекторов. Конечное Фурье-преобразование дифференциальных уравнений, описывающих коллектор, приводит к выражениям для параметров коллектора. Из-за погрешностей, в экспериментальном методе может быть использовано ограниченное число уравнений, определяемых особым выбором как временного интервала t_e, так и переменной Фурье ω. Характеристики коллектора можно определить методом наименьших квадратов, проводя только одну серию измерений при заданной температуре жидкости на входе. Результаты сопоставлены с данными, полученными при проведении большого количества серий измерений с различными значениями температуры жидкости на входе.